Influence of Excitation Energy on the Bacteriorhodopsin Photocycle

Richard W. Hendler,*,‡ Zsolt Dancsházy,§ Salil Bose,‡ Richard I. Shrager,∥ and Zsolt Tokaji§

Laboratory of Cell Biology, National Heart, Lung, and Blood Institute, and Division of Computer Research and Technology, National Institutes of Health, Bethesda, Maryland 20892, and Institute of Biophysics, Biological Research Center, Hungarian Academy of Sciences, Szeged, P.O. Box 521, H-6701 Hungary

Received November 2, 1993; Revised Manuscript Received January 25, 1994®

ABSTRACT: Kinetic curves for the bacteriorhodopsin (BR) photocycle were obtained both at 570 and at 412 nm at a series of increasing levels of intensity of the exciting laser. Singular value decomposition (SVD) of these curves showed two transitions in the kinetic profiles that occurred at specific levels of actinic light. This means that the photocycle was influenced by photon density in two ways. In a separate application of SVD, time-resolved optical spectra were analyzed at each of many levels of exciting laser intensities. The studies showed that the transition at the low level of laser intensity was due principally to an increase in the amount of BR that was turning over. The transition at the higher level of laser intensity showed a fundamental change in kinetics of the photocycle. At low intensity levels, the fast form of M (M_f) predominated, whereas at high levels the slow form of M (M_s) predominated. A distinction was found between M_f and M_s, in that the former decayed directly to the O intermediate whereas the latter decayed directly to BR.

It is known that the recovery of the ground state of bacteriorhodopsin (BR) following the activation of a photocycle by a laser pulse involves (at least) two forms of the M intermediate. The two forms have been referred to mostly as M_f and M_s, on the basis of the difference in time constants for the disappearance of the intermediates, the former being faster than the latter (Slifkin & Caplan, 1975; Lozier et al., 1976; Hess & Kuschmitz, 1977; Korenstein et al., 1979; Ohno et al., 1981; Hanamoto et al., 1984; Dancsházy et al., 1988; Kouyama et al., 1988; Ames et al., 1989). The ratio of M_f/M_s is highest at the lowest levels of laser activation intensity, and decreases as the intensity of the laser pulse increases.

There have been several explanations for the presence of fast and slow forms of M. One obvious possibility is the existence of different forms of BR. A very recent study by Eisfeld et al. (1993) using a combination of resonance Raman and optical transient studies has added support to the presence of heterogeneous forms of BR as the cause for fast and slow forms of M. Another view suggests that a homogeneous BR is susceptible to photocooperativity in which a single photon impinging on the basic BR trimer in the purple membrane causes the formation of M_f whereas two or more result in the formation of M_s [e.g., see Dancsházy and Tokaji (1993) and Tokaji (1993)]. A third view is favored by Varo, Lanyi, and collaborators, who have described two species of M which they call M_1 and M_2 (Varo & Lanyi, 1990, 1991a–c; Varo et al., 1990; Lanyi, 1993). The former is believed to be in reversible equilibrium with L and the latter with N. In this model, the phenomenological appearance of fast and slow forms of M is attributed to differences in kinetic constants for all of the equilibria involving M.

It is obvious that despite the efforts of extremely capable investigators employing the most sophisticated methods a generally accepted explanation for the existence of slow and fast forms of M has not been found. We have been interested in the perturbation of the ratio of M_f/M_s that is caused by a change in the intensity of actinic light which activates the cycle. In addition to trying to define the nature of this phenomenon, it may be possible to learn something about the fundamental basis for the existence of fast and slow forms of this key intermediate in the proton pumping cycle.

The most important findings of the current work are:

(1) Actinic light acts as a "titrant" on the photocycle kinetics, which exhibit two discrete transitions: one a simple linear increase in signal and the other a fundamental change in kinetics.

(2) M_f decays directly to the "O" intermediate prior to reestablishment of the ground state, whereas M_s decays directly to the ground state.

These findings are discussed within the framework of the major current views of the photocycle, which involve heterogeneity of BR, reversible equilibrium kinetics, and/or photocooperativity.

EXPERIMENTAL PROCEDURES AND ANALYSIS

Purple membranes (PM) were isolated according to standard procedures (Oesterhelt & Stoeckenius, 1974). The PM were sonicated for 1 min at 0 °C and embedded in a 10% acrylamide gel in the presence of 100 mM BTP (Bis-Tris propane) buffer, pH 7.0. The gels were then soaked for several days in the same buffer containing 1 M NaCl. Two different kinds of experiment were performed at pH 7 and ~25 °C on the BR sample. They will be referred to as type 1 and type 2 and will be described separately.

Type 1 Experiments. (A) Experimental Methods. These experiments were performed in Szeged, Hungary, and are described in detail elsewhere (Tokaji & Dancsházy, 1991; Dancsházy & Tokaji, 1993). A brief description will be included here. The actinic flashes were provided by an excimer laser pumped dye option containing coumarin 307 and LC 5000 (emission wavelength 505 nm, duration ~20 ns). Single-wavelength and transient kinetic data were acquired at the positions for maximum absorbance of bacteriorhodopsin (BR)

‡ Laboratory of Cell Biology, National Heart, Lung, and Blood Institute.
§ Hungarian Academy of Sciences.
∥ Division of Computer Research and Technology, National Institutes of Health.
® Abstract published in *Advance ACS Abstracts,* April 1, 1994.

0006-2960/94/0433-4604$04.50/0

at 570 or for the M intermediate at 412 nm, using a photomultiplier tube.

(B) Analytical Methods. Each data set contained 161 points in exponentially increasing time steps covering a range from 10^{-6} to ~0.3 s. The first 13 observations which contained the laser-induced bleaching of BR and buildup of the M intermediate were deleted, leaving 148 points containing the kinetics for the photocycle of BR. These points were logarithmically spaced with the first at 3.3 μs and the last at 273 ms. The time intervals increased from 0.25 μs in the beginning to 20 ms at the end. There were 15–17 data sets per experiment, with corresponding actinic flash intensities ranging over 3 orders of magnitude. The raw data were arranged as matrices with 148 rows and 15–17 columns. Each column in the type 1 experiment contains the kinetics (measured at a characteristic wavelength for either BR or M) at a particular level of light intensity. Call the matrix **A**, with elements $a_{i,j}$. The rows represent changes in kinetics caused by changes in light intensity. Thus, the $a_{i,j}$ element is the value of the absorbance at the ith time and the jth actinic flash intensity. These matrices were then analyzed by singular value decomposition (SVD) (Shrager & Hendler, 1982).

SVD is a linear algebra-based analytical procedure which separates the row and column spaces of matrices. It is able to extract a unique basis set of column space components (e.g., spectra or kinetic traces) from an input set of experimental data. It also produces a related basis set of row space components (e.g., titration or kinetic profiles). An explanation of SVD for those who do not have a background in linear algebra is presented in Hendler and Shrager (1993). It should be noted that in the SVD analyses of titrations described in the references cited, the columns contained optical spectra and the titrant was either pH or voltage. In the current application, the columns contain kinetic traces and the "titrant" is light.

Type 2 Experiment. (A) Experimental Methods. These experiments were performed at the NIH using a new type of ultra-rapid-scan multichannel spectrometer which is described separately (Cole et al., 1993; Hendler et al., 1993). The instrument has two spectrographs, each with a 46 photodiode array and capable of covering 130 nm of wavelength with a spectral resolution of 2.9 nm. Up to 512 spectra could be accumulated with a time resolution of anywhere from 10 μs to 21 s. Several hundred optical spectra were accumulated at appropriate time sequences for each of a series of actinic light flash intensities covering a range of 3 orders of magnitude. Time-averaging was accomplished by accumulating up to 1000 repeat series of time-resolved spectra at a time. The repetition rate for laser firing was 3.5 s. The zero time was set just after the time of the peak levels of BR bleaching and M-intermediate formation, where the rapid exponential changes of both components were evident. Thus, within each matrix **A**, the element $a_{i,j}$ was the absorbance at the ith wavelength and the jth time. In order to avoid bleaching of BR by the levels of monitoring light needed for the photodiode arrays, a lens system was used to spread the light over a large area on the cuvette and then to concentrate the beams before their entry into the spectrographs. Examination of the spectra prior to and after recovery from the actinic flash showed that this aim was achieved. Actinic flash intensity was constant within each matrix, but varied from matrix to matrix (i.e., a separate data matrix was accumulated at each of many different levels of actinic light intensity). The laser was a Neodymium YAG with a 5-ns pulse at 532 nm. The maximum energy applied to the sample per laser flash was 13 mJ/cm^2 or a total of 26 mJ.

(B) Analytical Methods. The raw data matrix for each level of light intensity contained 92 rows (wavelengths) and hundreds of columns (time points). SVD analysis was used to isolate specific time-resolved difference spectra and their associated time constants at each of a series of different discrete levels of actinic light.

Relation of Type 1 and Type 2 Experiments. The same BR preparation was used in the two types of experiment. In both cases, the BR was embedded in 10% acrylamide, and in the presence of 1 M NaCl at pH 7.0. The data pools, however, were quite distinct. Data for type 1 were collected using a photomultiplier tube. Data for type 2 were collected using two photodiode arrays. The kinds of SVD analyses applied in the two cases were different as described above. Two different kinds of laser were used, and the wavelength of the actinic pulse was 505 nm for type 1 and 532 nm for type 2. For both types of experiment, the relative strengths of the laser pulses were determined by monitoring the light reflected by transparent glass at each of the different intensities. The relative amounts of M_f and M_s in the type 1 experiments were determined from the amplitudes of the fast and slow exponentials in two-exponential fits to the columns of single-wavelength data. In the type 2 experiments, whole matrices of data accumulated at a given actinic light intensity were analyzed by SVD, and the peak amplitudes of the deduced difference spectra were used to quantify the amounts of M_f and M_s. In order to compare the individual amounts of M_f and M_s obtained as a function of light intensity in the two sets of data, the relative strengths of the two different laser sources must be estimated. The starting absorbance level for BR was ~0.3 absorbance unit at 570 nm for the type 1 experiments and ~0.3–0.5 for the type 2 experiments. Therefore, allowing for the difference in starting absorbances, the total amount of M produced (M_f and M_s) could be used as a relative measure of the two lasers. Using this index, it appears that the lowest level of light intensity in the type 1 experiment was about two-thirds that of the type 2 experiment and at the highest level the light intensity in the type 2 experiment was at least 4 times greater than that of the type 1 experiment.

Stockburger and co-workers have suggested a standardized calibration of the light energy input for the BR photolysis system based on relevant physical units (Schneider et al., 1989; Lohrmann et al., 1991; Eisfeld et al., 1993). They have defined a "photoconversion parameter" (pcp) which utilizes the quantum yield of the primary photochemical reaction, the cross section for the absorption of a photon by the parent species, the photon flux density of the source, and the length of the laser pulse. The advantage of pcp is that its negative represents the exponent (to the base e) for the extent of photolysis. Thus, pcp = 1 means a 63% probability for the photoconversion of BR. It can also be used to compare the effectiveness of different lasers for activating the BR photocycle. The maximum level of laser intensity for the type 1 experiment shown in Figures 1, 3, and 8 corresponds to a pcp value of 12. For the type 2 experiment shown in Figures 6 and 8, the maximum level of laser intensity corresponded to a pcp value of 80. Because the pcp is linearly related to total light flux, the relative units provided in the figures are readily convertible to the corresponding pcp using the maximum pcp values provided above. For example, the crossover point for the type 1 experiment shown in Figure 3 was at a relative laser flash intensity of $10^{-0.44}$ which corresponds to a pcp value of $10^{-0.44} \times 12 = 4.5$. For the type 2 experiment shown in Figure

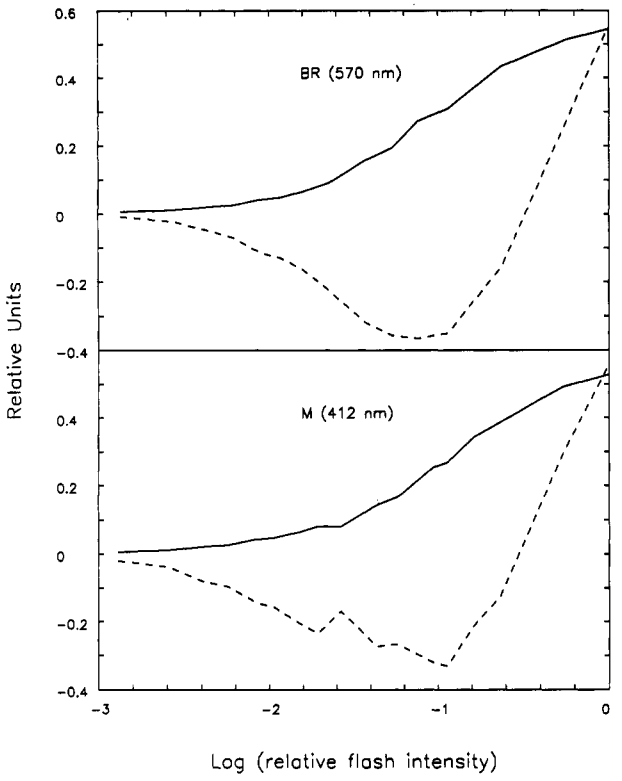

FIGURE 1: Time trace vectors obtained from SVD (i.e., columns of the V matrix) for the influence of actinic laser intensity on the kinetics of BR (570 nm) bleaching and recovery (top panel) and the kinetics of M intermediate (412 nm) generation and decay (bottom panel). The ordinate is in "distance" units as produced by SVD. The abscissa is on a log scale of relative laser light intensity. The flash intensity at 10° is equal to 12 pcp units. The solid lines represent column 1 and the dashed lines column 2 in the respective V matrices generated by SVD. See Experimental Procedures and Analysis for further details.

6, the crossover point occurred at a relative flash intensity near $10^{-1.25}$, which corresponds to a pcp value of $10^{-1.25} \times 80 = 4.5$. The photoconversion effectiveness of the two lasers, operating at different wavelengths, was essentially the same as indicated by the pcp values although the relative intensities of the laser sources were in the ratio of approximately $10^{1.25-0.44}$ or about 6 to 1.

RESULTS

Type 1 Experiment. When the kinetics of the decay of M and recovery of BR as functions of the level of laser light intensity were analyzed by SVD, it was found in both cases that the original data were of rank 2. For a case where the starting trace (i.e., the first column) is zero (in the absence of laser light, there are no kinetics), a rank 2 matrix means that the series of changes in light intensity produced two distinct effects on the system. Figure 1 shows the two significant titration vectors obtained by SVD (i.e., first two columns of the V matrix produced by SVD) for BR (top panel) and for the "M" intermediate (bottom panel). It is apparent that in both cases there were two "titrations" of the kinetics by light intensity: one in the range of 10^{-3}–10^{-1} of relative light intensity and the other in the range of 10^{-1}–10^{0}. The problem we discuss and resolve below is the definition of these two "titrations".

The simple increase in the amount of Br energized by an increase in laser energy without a fundamental change in kinetics would produce a series of kinetic curves (i.e., amplitude vs time) of increasing size but with no change in shape, yielding a rank 1 matrix with only one significant column in V. In

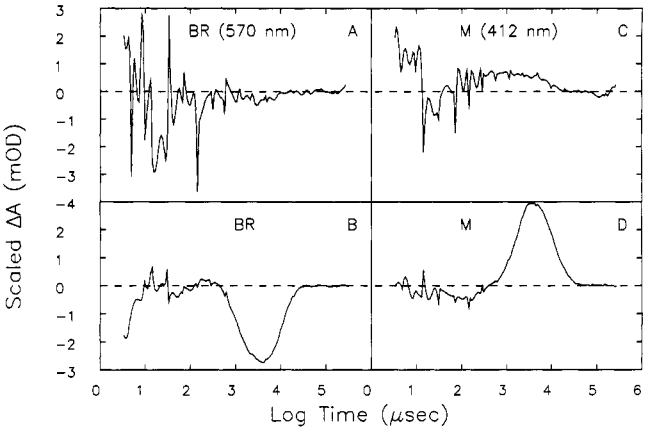

FIGURE 2: Difference kinetic traces for the experiments shown in Figure 1. Panel A shows the difference occurring over the range of relative laser flash intensity of $10^{-1.4}$–$10^{-2.9}$ for the BR experiment. Panel B covers the flash intensity range of 10^{0}–$10^{-0.94}$ for the BR experiment. Panel C shows the difference occurring over the range of relative laser flash intensity of $10^{-1.4}$–$10^{-2.9}$ for the M intermediate. Panel D covers the flash intensity range of 10^{0}–$10^{-1.0}$. Before a difference trace was taken, the weaker of the two traces was multiplied by a factor which normalized the magnitude of the maximum change in absorbance which occurred at 0.29 ms to that of the stronger trace. The ordinate is in "normalized" milli-OD units.

contrast, a change in the kinetics *per se* would alter the shape of the curve, yielding an A matrix of rank 2 or more. After normalization to equal magnitudes for the peak absorbance at the characteristic wavelength (i.e., 570 nm for BR), which occurred at 0.29 ms after the flash, difference kinetic traces were generated to cover each of the two ranges of laser intensity where changes were seen in Figure 1. These are shown in Figure 2. Figure 2A shows that for the first "titration" which occurred in the range of 10^{-3}–10^{-1} of relative light intensity, there was little change in the shape of the kinetic curve beyond the noise level, which is relatively high for the small signal evoked by the low-energy laser pulse. This shows that in the lower energy range of laser pulses, there was mainly a simple growth in the signal with no fundamental change in the kinetics of the photocycle. The same is seen for the "M" intermediate in the difference spectrum for the normalized kinetic curves obtained at 412 nm (Figure 2C). The "titrations" by light in the higher energy range (10^{-1}–10^{0}) are shown in Figure 2B,D. It is obvious that the signal to noise ratio is considerably higher in these figures than in Figure 2A,C. Although up to 1000 samples were averaged at the lower light intensities, it was impractical to achieve the same quality of signal because the lower signal was only $\sim 1/80$th that of the higher. These would require ~6400 repeats for each of the samples taken at the high intensity (i.e., more than 10^5 samples). Moreover, the change in kinetics caused by the higher light energy is clearly demonstrated by the results presented. Pronounced changes in the kinetics in the 1–10-ms time range are seen (Figure 2B,D). Figure 2B shows that the kinetics for both the bleaching and recovery of BR were affected. Figure 2D shows that the kinetics for both the generation and decay of the M intermediate were affected.

Each of the individual kinetic traces for the recovery of BR and the decay of the M intermediate, obtained at particular intensities of laser activation, could be readily modeled by a sum of two exponentials with time constants of ~1.7 ms (M_f) and ~6.2 ms (M_s) (Table 1). The relative percentages of M_f and M_s were drastically affected by the strength of the activation pulse, going from about 80% M_f at the lower energies of laser light to about 44% M_f at the highest energy pulse (Figure 3). The lifetimes of M_f and M_s were independent of

Table 1: Influence of Laser Light Intensity on Percentages and Lifetimes of M_f and M_s for Data of Type 1 Experiments

	M_f		M_s	
I (rel units)	tau[a] (ms)	%	tau (ms)	%
1.0	1.86	44	6.76	56
0.541	1.71	47	5.23	53
0.233	1.70	56	5.92	44
0.165	1.55	59	5.41	41
0.113	1.29	61	6.17	39
0.094	1.69	61	5.75	39
0.058	1.70	68	6.13	32
0.0435	1.74	68	6.45	32
0.0265	1.85	72	6.80	28
0.0193	1.76	72	6.54	28
0.0151	1.81	72	6.85	28
0.0106	1.68	72	6.45	28
0.0083	1.69	76	6.58	24
0.0057	1.78	69	6.76	31
0.00414	1.72	74	6.85	26
0.0026	1.54	71	6.62	29
0.0013	1.52	80	6.76	20

[a] Tau is the time constant, which is the reciprocal of the kinetic constant.

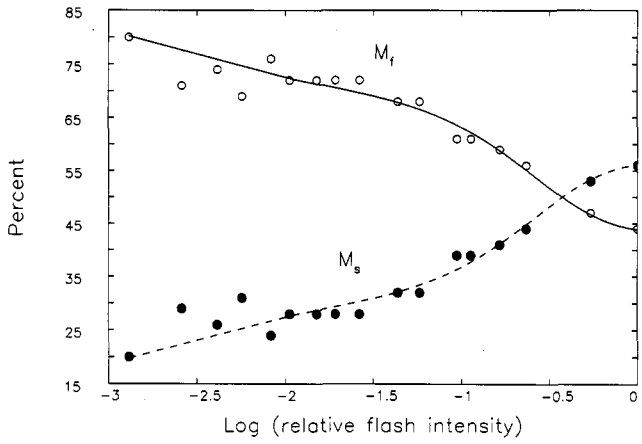

FIGURE 3: Percents of M_f and M_s (compared to the sum of M_f + M_s) as functions of relative actinic light intensity for the data of the experiment shown in Figures 1 and 2. The flash intensity at 10^0 is equal to 12 pcp units. The amplitudes of absorbance at 412 nm were fit to two exponentials: one with a time constant of ~1.7 ms and the other ~6.2 ms. The actual time constants and proportion of M_f at each level of light intensity are shown in Table 1. The solid and dashed lines in the figure were obtained using the saturation equation in the text with the fitted constants shown in Table 2, columns 2 and 3.

the exciting light intensity (Table 1). In this figure, the solid and dashed lines are the results of computer fittings based on saturation curves for the activation of M_f and M_s (described below). The data points show that in the lower range of laser intensity, where the magnitude of the change was linear with flash intensity, there was little change in the proportion of M_f to M_s. It should be pointed out that because of the small magnitudes of the changes occurring at the lowest levels of light intensity, the calculated percents of M_f and M_s at these levels are subjected to greater error. The major rates of change with respect to light intensity occurred in the latter part of the curves. This is consistent with the results of the SVD analysis and difference spectra shown in Figures 1 and 2.

Type 2 Experiment. In order to obtain more information on the nature of the photocycle transitions involving M_f and M_s, SVD was again used, but in a different way as described under Experimental Procedures and Analysis. This time, entire optical absorption spectra were analyzed as a function of time for each of a series of different energy laser pulses. The data were resolved mostly as rank 2 with respect to time.

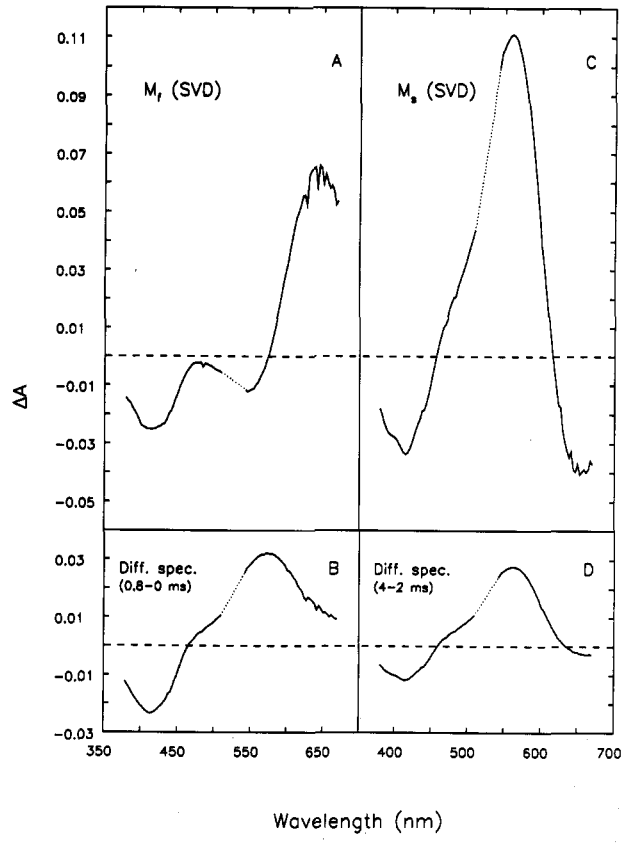

FIGURE 4: SVD-derived and local difference spectra for time-dependent spectral changes associated with M_f and M_s. Panel A was derived from SVD for M_f (T ~1.1 ms) and panel C for M_s (T ~3.5 ms). Panel B is a local difference spectrum (0.8–0 ms), and panel D is the local difference spectrum for 4–2 ms. The three arrows in each panel are at 412, 570, and 640 nm, respectively. The spectrometer system utilizes two spectrographs. For these experiments, one covered the range from 379.3 to 509.7 nm and the other from 542.8 to 670.3 nm. The dotted portion in each spectrum represents the gap from 509.7 to 542.8 nm. The level of relative laser flash intensity for this experiment $10^{-0.72}$ (refer to Figure 6).

In some cases, a rank of 3 or 4 was found, but the two primary transitions were always present. A representative difference spectrum, resolved by SVD, for the faster of the two principal transitions (time constant = ~1.1 ms), is shown in Figure 4A. A local difference trace for this time period, obtained from the raw data (0.8–0 ms), is shown in Figure 4B. The difference traces for the transition of M_s are shown in Figure 4C (SVD) and Figure 4D (raw data, 4–2 ms). For the BR photocycle where all of the components have spectrally separated peaks, the negative troughs show what is decaying and the positive peaks show what is being generated. This implies that the decaying and generated species share the same time constant. The isolated difference trace obtained by SVD (panel A) shows that as M_f disappears (at 412 nm) there is no concomitant formation of BR (at 570 nm). Instead there is a concomitant formation of a peak at ~640 nm, which is characteristic of the O intermediate (Zimanyi et al., 1989). It is also interesting that a peak near 550 nm is also diminishing. This position has been attributed to the N intermediate (Kouyama et al., 1988). A striking difference is seen in the difference spectrum for M_s generated by SVD (panel C). As M_s disappears (at 412 nm), there is a concomitant generation of BR (at 570 nm). There is no generation of O (at ~640 nm). Instead, the peak at ~640 nm is decaying at the same rate as M_s. This figure also demonstrates the power of the SVD method of deconvolution. Figure 4A,C shows SVD-resolved difference spectra for individual transitions. Actual

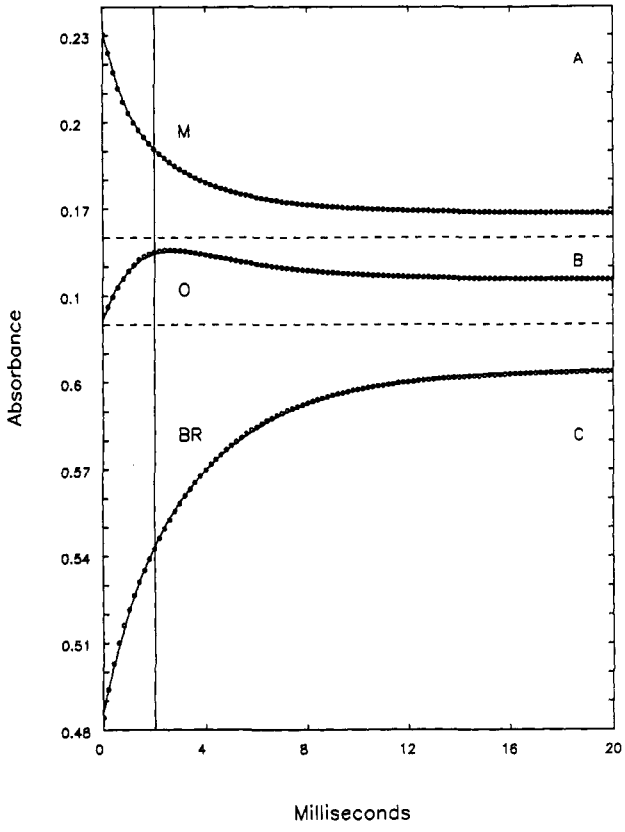

FIGURE 5: Single-wavelength kinetics for the experiment shown in Figure 4. The points show the absorbances at 411, 641, and 569 nm, respectively in panels A, B, and C. The units on the y axis are appropriate individually for each panel. For example, the base-line values for panels A, B, and C are 0.16, 0.09, and 0.48, respectively. The lines show computer fits using a model of two exponentials. The fitted time constants (in milliseconds) were 0.98 and 3.5 for "M", 1.4 and 3.2 for "O", and 0.96 and 3.7 for "BR". For display purposes, every other data point has been discarded. The vertical line represents 2 ms.

difference spectra shown in Figure 4B,D contain an overlap of the two transitions. The only evidence in the difference spectra for the involvement of the "O" intermediate in the conversion of M_f but not M_s is in the positive absorbances around 640 nm in panel B, and the negative absorbances in this spectral region in panel D. Other evidence for the direct conversion of M_f to O and of M_s to BR is presented in Figure 5. The changes in absorbance at 411 nm (M), 641 nm (O), and 569 nm (BR) during the first 20 ms are shown in panels A, B, and C, respectively. The lines in the three panels are "best fits" using the sum of two exponentials. In all cases, the fast exponential corresponded to a time constant of ~1 ms and the slower to ~3.5 ms. The vertical line is at 2 ms. It is seen that the fast decay of M is coincident with the fast rise of O. The decay in O is coincident with the slow decay of M, an observation that supports the view that M_s does not decay to O. BR also shows the same two time constants. The decay of M_f represented 48% of the total M signal, but the recovery of the fast component of BR represented only 16% of the total amount of BR bleaching. This observation is consistent with the view that M_f decays first to O, rather than directly back to BR. The changes in relative amounts of M_f and M_s as functions of laser energy are shown in Figure 6. In the range of laser flash intensity used for this series of experiments, the proportion of M_f decreases from ~70% to ~38%.

The individual responses of M_f and M_s to increasing laser flash energy are shown in Figure 7 for the experiments depicted in Figures 1–3, where the data were collected at 412 nm only.

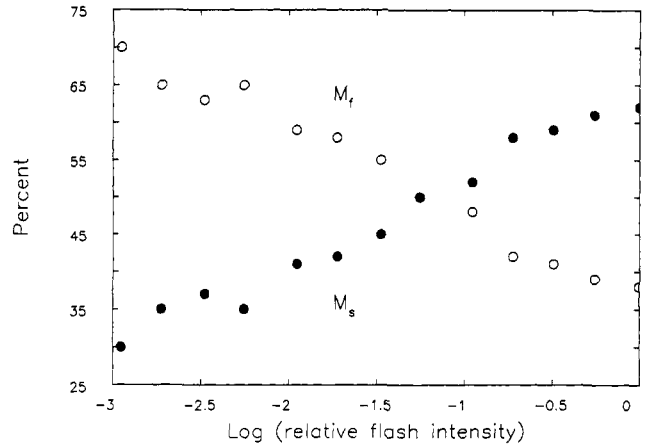

FIGURE 6: Relative percents of M_f and M_s (compared to $M_f + M_s$) as a function of laser light intensity. The amplitudes at 570 and 412 nm were measured in the SVD-derived difference spectra for each level of light intensity. The flash intensity at 10^0 is equal to 80 pcp units.

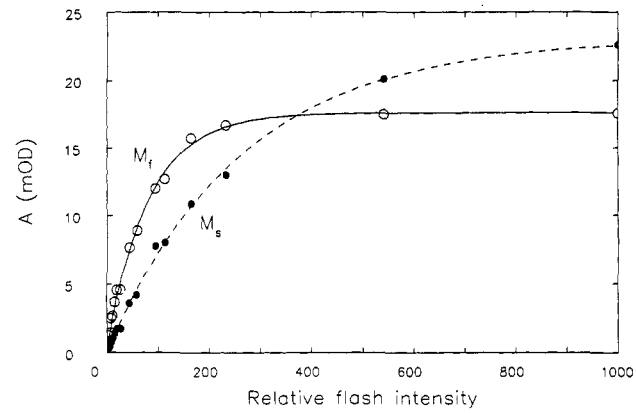

FIGURE 7: Actual amplitudes of absorbance for M_f and M_s obtained by fitting the 412-nm data in the experiments shown in Figures 1–3 to two exponentials, as described in the text. The points show the actual data, and the lines are simulations based on the saturation equation in the text and the fitted parameters in Table 2, columns 2 and 3. The starting (i.e., ground state) optical density for BR was 0.3. The relative flash intensity, 1000, equals 12 pcp units.

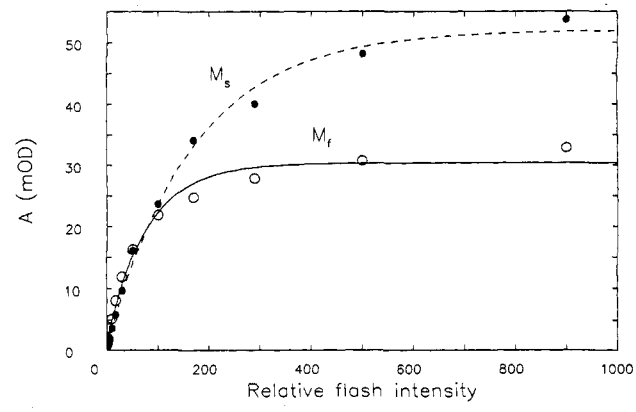

FIGURE 8: Actual amplitudes of absorbance for M_f and M_s obtained by fitting the 412-nm data in the experiments shown in Figures 4 and 5 to two exponentials, as described in the text. The points show the actual data, and the lines are simulations based on the saturation equation in the text and the fitted parameters in Table 2, columns 4 and 5. The starting (i.e., ground state) optical density for BR was 0.41. The relative flash intensity, 1000, equals 80 pcp units.

Figure 8 shows the data for the amplitudes of the signal at 412 nm in the spectra obtained in the SVD analysis of the experiments depicted in Figures 4–6. In both Figure 7 and Figure 8, the experimental data are shown as points. The

Table 2

	Figure 6 expt		Figure 7 expt	
fitted parameter	M_f	M_s	M_f	M_s
A	17.147	23.027	28.89	51.22
tau[a] (I)	82.79	266.4	78.19	169.5

[a] Tau is analogous to a time constant (see Table 1), where, however, the independent variable is flash intensity (I) rather than time.

trends for all of the M's in these figures resemble saturation curves. The lines shown in the figures are best fits to the saturation equation:

$$\text{amplitude} = A[1 - \exp(-kI)] + d$$

where $A + d$ is the amplitude at infinite light intensity, k is the equivalent of a kinetic constant in terms of I, the intensity of the laser flash (rather than time), and d is the value at $t = \infty$. The values of all of the fitted parameters are shown in Table 2. It is seen that within the accuracy of the experimental data, the curves based on saturations of two populations of M intermediates can provide adequate fits.

DISCUSSION

The current studies have involved SVD in two different kinds of application. It is important to note the difference in the two approaches. The first application analyzed, directly, the effects of the actinic laser intensity, as a titrant, on the kinetics of the BR photocycle. The columns of the input matrix were kinetic curves (i.e., amplitude vs time) at either 570 nm for BR or 412 nm for the M intermediate. The rows recorded the influence of light on these kinetics. The raw data were found to be of rank 2. This means that there were two kinds of changes caused by modulation of light flux. The changes in the lower range of light intensity were mainly due to an increase in the magnitude of BR cycling, with little change in the kinetics of the photocycle. The second change at the higher level was associated with fundamental changes in the turnover kinetics of both BR and the M intermediate.

The second application of SVD analyzed the kinetic changes of the optical spectra for the various intermediates of the BR photocycle. The columns of the input matrix were optical spectra, and the rows were changes in optical absorbance as a function of time. A completely different experiment was performed at each of many different levels of laser flash intensity. Two principal time-dependent transitions were found by SVD at each level of light intensity. These two are not the same as the two found in the first application, which were light intensity-dependent changes. Each of the two transitions in the second application has a unique time constant. The same two time constants were found at each level of light intensity, but the relative proportion of the faster (i.e., M_f) to the slower (i.e., M_s) decreased with increasing light intensity. One of the most striking findings of the SVD analysis in the second application, and confirmed by computer-fitting of the raw data at characteristic single wavelengths, is that under the conditions of these experiments M_f decays directly to the O intermediate whereas M_s decays directly back to BR. This conclusion is inferred directly from the data and does not depend on any assumptions.

In spite of the many differences in the two types of experimental protocol used in the current studies, it is seen in Figures 3 and 6 that the relative yields of M_f and M_s as functions of increasing light intensity are quite comparable. In comparing the absolute yields of M_f and M_s as functions of increasing light intensity, it is important to note (see Experimental Procedures and Analysis) that the laser intensity used in the type 2 experiment was considerably above that used in the type 1 experiment. In comparing Figures 7 and 8, it is seen that the crossover point for the amounts of M_f and M_s occurred at a level of 35–40 mOD units of M produced in both cases. As pointed out under Experimental Procedures and Analysis, this crossover point corresponds to ~4.5 pcp units in both experiments.

The existence of two forms of the M intermediate, M_f and M_s, has been known for almost 20 years (see the introduction). There are, at present (at least), four competing views, not necessarily mutually exclusive, on the meaning of this finding. One (i.e., heterogeneity) is that (at least) two basically different populations of BR are present, with different quantum efficiencies and different saturation levels. M_f would be associated with one and M_s with the other. Another view (i.e., cooperativity) is that one population is present but that there is a cooperative effect of light so that multiple photon hits on a target (i.e., the BR trimer) lead to the formation of M_s, and single hits to M_f. A third view (i.e., equilibration) is that in a homogeneous BR population there are two forms of M (M1 and M2), each of which is in reversible equilibrium with its nearest kinetic neighbor (L ↔ M1 ↔ M2 ↔ N). The phenomenological appearance of M_f and M_s then reflects the values of the individual kinetic constants. Thus, a high back-reaction for N → M2 would increase the τ for M2 decay [e.g., see Varo and Lanyi (1991b)]. A fourth possibility (suggested by Stockburger) is that during the time of the laser flash (5–20 ns) the K intermediate is susceptible to a direct phototransition to M_s. Therefore, the higher the laser intensity, the greater the formation of M_s. In a separate paper (Shrager et al., unpublished experiments), we will consider the four possible explanations listed here in greater detail.

The results of the application of SVD to kinetic profiles obtained at increasing levels of actinic light strengthen the view that light flux *per se* has a specific and quantitative effect on photocycle kinetics. An analogy of light as a "titrant" of photocycle kinetics seems appropriate. The heterogeneity, cooperativity, and K-phototransition models can account for this ability of activation light to alter the distribution of M_f and M_s. In the equilibration model, which is based on a homogeneous photocycle, some specific mechanism for photocooperativity to influence the relevant kinetic constants must be formulated.

The second finding in the present paper is that M_f decays directly to O and that both M_s and O decay directly to BR. The inclusion of the N intermediate is discussed below. The observation on M_f decay is inherently compatible with separate photocycles which involve different intermediates. For the homogeneous cooperative model, it must be proposed that the single photon-energized BR proceeds through a cycle in which $M_f \rightarrow O \rightarrow BR$, whereas the multiple photon-energized BR proceeds through a cycle in which $M_s \rightarrow BR$, with a similar τ as that for $O \rightarrow BR$. For the equilibration model, as presented in Varo and Lanyi (1991b), some additional postulations appear to be required. At low light fluxes, a direct shunt from M1 to O could explain the finding that $M_f \rightarrow O \rightarrow BR$. The alternative route of M1 → M2 ↔ N ↔ O → BR would have to involve rapid equilibration between M2 and O, so that both intermediates would decay to BR with the same apparent τ. A somewhat more elaborate form of the equilibration model has recently been presented (Lanyi, 1993). With similar modifications as described above, this model could also be compatible with the findings in the present paper.

Our results fit very closely with some of the findings in a new study published by Eisfield et al. (1993). Using a combination of resonance Raman and optical transient spectroscopy, they have concluded that a quite heterogeneous population of BRs exists. Approximately 50% is proposed to have the ability for L to decay to BR through M and the other to decay to BR without forming M. In each of these two categories, different specific decay patterns are promoted at different pHs. At neutral pH, three individual pathways should be present: (1) $M_f \rightarrow O \rightarrow BR$; (2) $M_s \rightarrow BR$; and (3) $M_f \rightarrow N \rightarrow BR$. We have already discussed our independent conclusions for pathways 1 and 2. Examination of the SVD-deduced difference spectrum involving M_f (Figure 4A) shows that an N-like spectral component decays to BR on the same time scale as does M_f. This would be the expected finding if the τ for N decay in pathway 3 was close to that of M_f decay in pathway 2. These data provide no confirmation for the direct formation of N from M_f shown in pathway 3. If an $M_f \rightarrow N$ conversion does occur, this process would precede the kinetic event resolved by SVD in Figure 4A. Our analyses have not resolved this possible earlier event.

Although our results confirm the ability of light flux to influence the photocycle and give evidence of the specific quantitative and qualitative nature of this effect, they do not decide the question of which of the various possible models is valid. As we have discussed above, the multichannel data and SVD analyses used in the current studies strongly support the conclusion that only M_f decays directly to the O intermediate. It must be noted, however, that other studies by Luchian and two of the present authors (Zs. Dancsházy and Zs. Tokaji) using single-wavelength data and different analytical techniques have arrived at a quite different conclusion, namely, that both M_f and M_s decay to the O intermediate (Tokaji et al., 1993).

REFERENCES

Ames, J. B., Fodor, S. P. A., Gebhard, R., Raap, J., Van der Berg, M. M., Lugtenburg, J., & Mathies, R. A. (1989) *Biochemistry 28*, 3681–3687.

Dancsházy, Zs., & Tokaji, Zs. (1993) *Biophys. J. 65*, 823–831.

Dancsházy, Zs., Govindjee, R., & Ebrey, T. G. (1988) *Proc. Natl. Acad. Sci. U.S.A. 85*, 6358–6361.

Eisfeld, W., Pusch, C., Diller, R., Lohrmann, R., & Stockburger, M. (1993) *Biochemistry 32*, 7196–7215.

Hanamoto, J. H., Dupuis, P., & El-Sayed, M. A. (1984) *Proc. Natl. Acad. Sci. U.S.A. 81*, 7083–7087.

Hendler, R. W., & Shrager, R. I. (1994) *J. Biochem. Biophys. Methods 28*, 1–33.

Hendler, R. W., Bose, S. K., & Schrager, R. I. (1993) *Biophys. J. 65*, 1307–1317.

Hess, B., & Kuschmitz, D. (1977) *FEBS Lett. 74*, 20–24.

Korenstein, R., Hess, B., & Markus, M. (1979) *FEBS Lett. 102*, 155–161.

Kouyama, T., Nasuda-Kouyama, A., Ikegami, A., Mathew, M. K., & Stoeckenius, W. (1988) *Biochemistry 27*, 5855–5863.

Lanyi, J. K. (1993) *Biochim. Biophys. Acta 1183*, 241–261.

Lohrmann, R., Grieger, I., & Stockburger, M. (1991) *J. Phys. Chem. 95*, 1993–2001.

Lozier, R. H., Bogomoini, R. A., & Stoeckenius, W. (1975) *Biophys. J. 15*, 955.

Lozier, R. H., Niederberger, R. A., Bogomolni, R. A., Hwang, S. B., & Stoeckenius, W. (1976) *Biochim. Biophys. Acta 440*, 545–556.

Oesterhelt, D., & Stoeckenius, W. (1974) *Methods Enzymol. 31*, 667–679.

Ohno, K., Takeuchi, Y., & Yoshida, M. (1981) *Photochem. Photobiol. 33*, 573–578.

Schneider, G., Diller, R., & Stockburger, M. (1989) *Chem. Phys. 131*, 17–29.

Shrager, R. I., & Hendler, R. W. (1982) *Anal. Chem. 54*, 1147–1152.

Slifkin, M. A., & Caplan, S. R. (1975) *Nature 253*, 56–58.

Tokaji, Zs. (1993) *Biophys. J. 65*, 1130–1134.

Tokaji, Zs., & Dancsházy, Zs. (1991) *FEBS Lett. 281*, 170–172.

Tokaji, Zs., Dancsházy, Zs., & Luchian, T. (1993) *Int. Biophys. Congr., 11th, Abstr.* E2.29, p 198.

Varo, G., & Lanyi, J. K. (1990) *Biochemistry 29*, 2241–2250.

Varo, G., & Lanyi, J. K. (1991a) *Biochemistry 30*, 5008–5015.

Varo, G., & Lanyi, J. K. (1991b) *Biochemistry 30*, 5016–5022.

Varo, G., & Lanyi, J. K. (1991c) *Biophys. J. 59*, 313–322.

Varo, G., Duschl, A., & Lanyi, J. K. (1990) *Biochemistry 29*, 3798–3804.

Zimanyi, L., Keszthelyi, L., & Lanyi, J. K. (1989) *Biochemistry 28*, 5165–5172.